Conversion of Talc into Silica Nanoparticles via Thermal and Chemical Treatment

Klaudia Simanová[1*)], Slavomír Hredzák[2)], Inna Melnyk[3)]

[1*)] Institute of Geotechnics of SAS, Watsonova 45, 040 01 Košice, Slovak Republic, simanova@saske.sk; https://orcid.org/0009-0007-9001-9379
[2)] Institute of Geotechnics of SAS, Watsonova 45, 040 01 Košice, Slovak Republic, hredzak@saske.sk; https://orcid.org/0000-0001-6802-9684
[3)] Institute of Geotechnics of SAS, Watsonova 45, 040 01 Košice, Slovak Republic, melnyk@saske.sk; https://orcid.org/0000-0002-2559-5771

https://doi.org/10.29227/IM-2026-02-02-016

Submission date: *2026-28-08* | Review date: *2026-07-09*

Abstract

The development of efficient and economically viable adsorbents is of increasing importance for the removal of pollutants from aqueous systems. Among the various materials investigated for adsorption applications, silica-based materials have attracted considerable attention due to their high specific surface area, tunable pore structure, chemical stability, and the presence of surface silanol groups, which can participate in adsorption processes or serve as sites for further surface functionalization. These properties make silica particularly promising for the removal of heavy metals, dyes, and other inorganic and organic pollutants from water. Despite these advantages properties, the preparation of high-purity nanoscale silica commonly relies on relatively expensive synthetic precursors and may involve multistep processes, high energy consumption, and the use of chemicals with a substantial environmental impact. Therefore, increasing attention has been directed toward the utilization of naturally occurring silica-rich materials, industrial by-products, and waste-derived resources as alternative precursors for silica production. Such approaches can reduce dependence on costly conventional raw materials while simultaneously contributing to resource conservation and waste valorization. Natural mineral resources represent a particularly interesting alternative because of their abundance, relatively low cost, and high content of inorganic constituents suitable for further processing. Talc ($Mg_3Si_4O_{10}(OH)_2$) is a silica-containing magnesium silicate mineral that can therefore serve as a potential precursor for the production of silica-based materials. Through appropriate thermal and chemical treatment, magnesium and other mineral components can be removed or transformed, enabling the recovery of silica and its subsequent conversion into nanoscale adsorbent materials. The valorization of talc in this manner could provide an alternative route to silica production while increasing the value of this abundant mineral resource. In our work we focused on the preparation of silica from a readily available SiO_2-rich mineral and the subsequent modification of the resulting silica surface to develop adsorbents for the removal of inorganic and organic pollutants from wastewater. At this stage, talc was used as the SiO_2 source. The talc was ground to a particle size of ≤100 μm and subsequently subjected to thermal treatment. The treated powder was then used for the preparation of silica via a two-step synthesis. The first step involved leaching with hydrochloric acid, which removed impurities and metal cations from the material. In the second step, the material was leached with sodium hydroxide, followed by the precipitation of SiO_2 through neutralization. The prepared silica was subsequently characterized. The characterization results confirmed the successful preparation of pure, amorphous silica with a particle size of approximately 100 nm.

Keywords: *talc, leaching, mineral processing, silica, nanoparticles*

1. Introduction

The increasing occurrence and diversity of contaminants in aquatic environments have created a growing need for reliable and cost-effective technologies for their removal. Wastewater may contain complex mixtures of inorganic and organic substances, including heavy metal ions, dyes, aromatic compounds, pharmaceutical residues, and other potentially hazardous pollutants [1,2]. The wide variation in their charge, polarity, molecular size, solubility, and chemical stability makes both the simultaneous removal of chemically diverse contaminants and the selective removal of individual target compounds particularly challenging. Therefore, considerable attention has been devoted to the development of solid materials capable of binding contaminants through physical or chemical interactions. A wide range of materials has been investigated for adsorption applications, including activated carbons, zeolites, clay minerals, metal oxides, polymeric materials, and silica-based compounds [1-3]. Their adsorption performance is strongly influenced by parameters such as specific surface area, pore structure, surface charge, and the nature and accessibility of functional groups. Depending on the adsorbent-adsorbate system, contaminant uptake may involve electrostatic attraction, ion exchange, surface complexation, hydrogen bonding, hydrophobic interactions, or a combination of these mechanisms [1-5]. Although many conventional adsorbents exhibit high removal efficiencies, their practical application may be limited by factors such as production cost, regeneration requirements, limited selectivity, difficult separation from the treated medium, or insufficient affinity for particular types of pollutants [1,2]. This has encouraged the development of adsorbents whose surface chemistry can be deliberately adjusted according to the properties of the targeted contaminant. Silica-based materials are particularly attractive for this purpose because of their chemical stability, adjustable textural properties, and the presence of surface silanol groups that enable further chemical modification [3-5]. The resulting silica-organic interface can introduce new contaminant-binding sites while preserving the stable inorganic framework. Organosilanes are frequently used as coupling agents for this purpose, as their hydrolysable alkoxy groups react with surface silanols to form stable siloxane bonds, whereas their organic moieties introduce the required chemical functionality [4,5,6]. Depending on the structure of the organosilane, the modified surface can exhibit different

affinities for metal ions and for ionic, polar, or non-polar organic compounds. For example, thiol-functionalized silica has demonstrated enhanced affinity for Pb(II) ions [7], whereas modified silica obtained from rice husk has been successfully applied to dye adsorption [8]. Moreover, surface functionalization can influence not only adsorption but also the aggregation, flocculation, and sedimentation behaviour of silica nanoparticles in wastewater matrices [9].

The development of multifunctional silica adsorbents is therefore important not only for improving adsorption capacity but also for controlling surface selectivity and tailoring material properties for specific applications. Understanding the relationship between the chemical structure of the surface modifier and the resulting adsorption behaviour is essential for the rational design of materials suitable for the treatment of chemically complex wastewater [3-7]. At the same time, the cost and environmental impact of the silica precursor should be considered. The use of abundant natural minerals or waste-derived silica sources may reduce dependence on conventional synthetic precursors and contribute to the development of more economically viable adsorbent materials [8,10].

In the present study, talc was selected as an alternative mineral-derived silica source. The mineral was obtained from the talc-magnesite deposit located near the village of Gemerská Poloma in the Rožňava District of the Košice Region, Slovakia [11]. Pure talc has the chemical formula $Mg_3Si_4O_{10}(OH)_2$, corresponding, when expressed as oxide equivalents, to approximately 63 wt.% SiO_2, 32 wt.% MgO, and 5 wt.% H_2O [11,12]. Natural talc, however, is rarely present as a completely pure mineral phase. Talc from the Gemerská Poloma deposit may be associated with quartz, dolomite, chlorite, and minor pyrite, while its composition may also include small amounts of iron- and aluminium-containing constituents [11]. Preliminary compositional analysis of the material used in this study likewise indicated the presence of Fe- and Al-containing impurities.

Therefore, a multistep treatment procedure was selected for the preparation of high-purity SiO_2 nanoparticles, with the aim of removing magnesium-containing phases and accompanying mineral impurities. The procedure included thermal pretreatment, acid leaching, alkaline extraction of silica, and its subsequent precipitation from the resulting silicate solution. Similar acid-leaching and extraction approaches have previously been applied to obtain silica-rich and porous materials from talc and other naturally occurring silicate minerals [10,12]. The prepared samples were characterized using powder X-ray diffraction (XRD), X-ray fluorescence (XRF) spectrometry, scanning electron microscopy (SEM), and nitrogen adsorption-desorption measurements. These methods were used to evaluate the phase composition, chemical purity, particle morphology, and textural properties of the obtained silica. The resulting material is intended to serve as a silica support for subsequent surface functionalization with organosilanes and the development of adsorbents for inorganic and organic water contaminants.

2. Methods

The preparation of silica from talc consisted of multistep synthesis. In the first step, the material was grounded in a planetary ball mill Pulverisette 6 (Fritsch, Germany) for 25 minutes at 550 rpm to obtain particles of size of ≤100 µm. The resulting powder was subsequently thermally treated in a muffle furnace CE 4 (Celsius KFT, Hungary) at 680 °C for 3 h and thereby activating the sample. The activated sample was then leached in 4 M hydrochloric acid solution (35%, p.a., CentralChem) at a liquid-to-solid ratio (L/S) of 10 and continuously stirred for 3 h at 80 °C. The resulting samples were filtered, washed with distilled water, and used in the subsequent step, which involved leaching in a 6 M NaOH (≥98.0%, p.a., mikroCHEM) solution for 24 h at 90 °C. During this step, the silica was dissolved in the alkaline solution in the form of sodium silicate, which remained in the filtrate after filtration. The filtrate was acidified to neutral pH, resulting in the formation of a silica gel. The silica gel was left to age for 24 h and was then filtered and dried at 80 °C for 24 h to obtain SiO_2.

Powder X-ray diffraction patterns were recorded on a Bruker D8 Advance diffractometer (Germany) using Cu $K\alpha_1$ radiation at 40 kV and 40 mA. Data were acquired within a 2θ range of 5–80° using a step size of 0.01° and a counting time of 4 s per step.

The bulk concentrations of Si and selected metals in the mineral samples were measured by ICP-MS using an Agilent 7700 instrument (Agilent Technologies, USA).

The semi-quantitative oxide composition was additionally evaluated by ED-XRF using a SPECTRO XEPOS III spectrometer (SPECTRO Analytical Instruments GmbH, Germany) and the TurboQuant-Pellets method. The results were expressed in wt.%.

Surface morphology and local elemental composition were examined using a MIRA 3 field-emission scanning electron microscope (TESCAN, Czech Republic) coupled with an energy-dispersive X-ray detector (Oxford Instruments, UK). The specimens were mounted on conductive carbon tape and coated with a 3 nm carbon layer to minimize charging. Images were acquired at magnifications of 2.0 k× for the starting mineral and 50.0 k× for the prepared and modified silica samples. EDX measurements were performed at three different areas of each sample, and the results were reported as mean values with standard deviations.

Specific surface areas were calculated from N_2 adsorption–desorption isotherms recorded at −196 °C using an Autosorb 6100 surface area and pore size analyzer (Anton Paar, Austria). Before analysis, the samples were degassed at 100 °C for 24 h under vacuum (<2 Pa). The BET equation was applied to the adsorption data within a relative pressure range of P/Po = 0.05–0.35. The total pore volume (V_{tot}) was estimated from the amount of N_2 adsorbed near saturation.

3. Results and Discussion

According to literature data on the talc deposit near Gemerská Poloma, the investigated mineral could contain talc, magnesite, dolomite, chlorite, pyrite, graphite, and quartz. However, XRD analysis identified only some of these mineral phases in the studied sample. The measured XRD patterns are presented in Fig. 1. For the original ground talc sample (Fig. 1a), reflections assigned to talc (Tlc), the dominant crystalline phase, were observed together with those of dolomite (Dol), chlorite (Chl), and minor graphite (Gr). No distinct reflections attributable to magnesite, pyrite, or quartz were detected, indicating that these phases were either absent, present below the XRD detection limit, or obscured by overlapping reflections. In the thermally treated sample (Fig. 1b), talc remained the dominant phase, while reflections of chlorite, dolomite, and minor graphite were also detected. After HCl leaching, the sample exhibited only reflections attributable to talc within the detection limit of the method (Fig. 1c). The positions and widths of the principal talc reflections remained essentially unchanged in the patterns, indicating that the thermal and acid treatments did not markedly disrupt its crystalline structure.

Following alkaline extraction with NaOH and subsequent silica precipitation, the resulting SiO_2 sample (Fig. 1d) displayed a broad diffuse halo centred at approximately 2θ = 22°, with no sharp Bragg reflections. This pattern is characteristic of X-ray-amorphous silica and indicates the absence of detectable crystalline impurities.

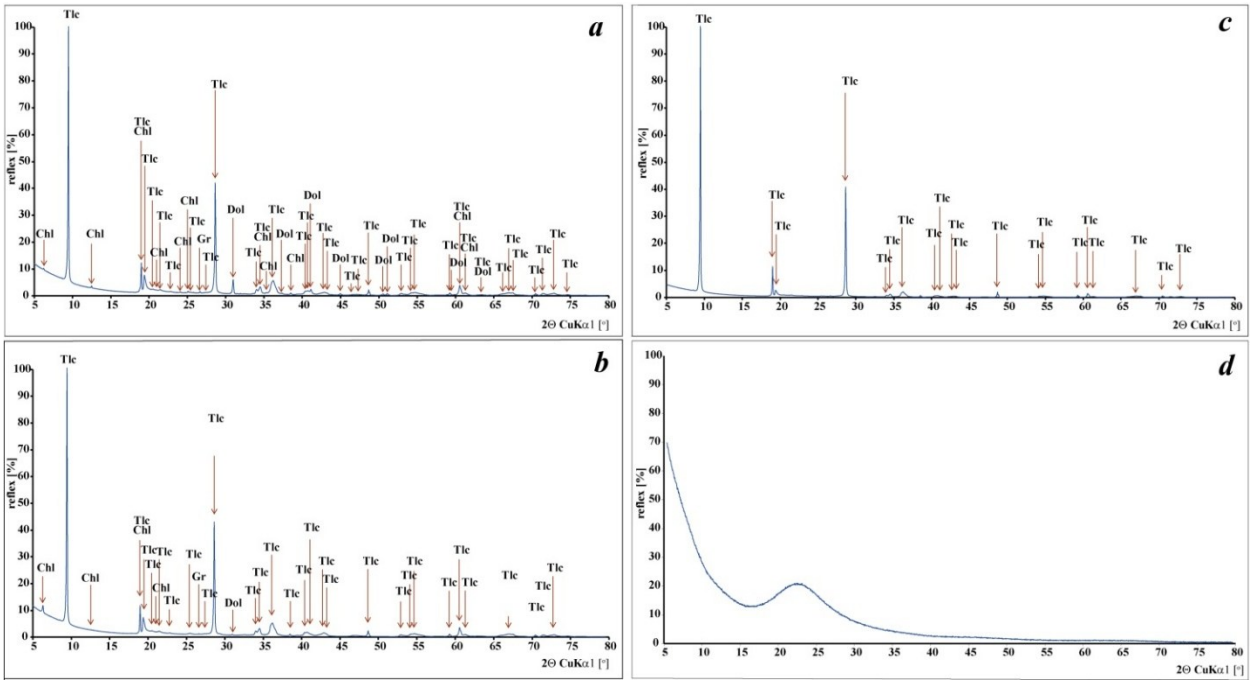

Fig. 1. Diffractograms of the samples: a – talc after grinding, b – talc after thermal treatment, c – talc after leaching in HCl, d – prepared silica (SiO_2).

The semi-quantitative oxide composition of the initial talc sample was determined by ED-XRF, and the major constituents are summarized in Table 1 (the values represent semi-quantitative, non-normalized ED-XRF results. Only the major oxide constituents are presented). The sample contained predominantly SiO_2 (64.41 wt.%) and MgO (32.65 wt.%), together with smaller amounts of CaO (2.46 wt.%), Fe_2O_3 (1.05 wt.%), and Al_2O_3 (0.38 wt.%). The calculated molar MgO/SiO_2 ratio was approximately 0.76, which is close to the theoretical value of 0.75 for talc ($Mg_3Si_4O_{10}(OH)_2$) and supports its identification as the dominant mineral phase. The presence of CaO is consistent with the dolomite detected by XRD, whereas the Fe- and Al-containing components may be associated with chlorite and other minor mineral impurities. Thus, the ED-XRF results complement the XRD analysis and confirm the predominance of talc in the initial mineral sample.

Tab. 1. Percentual composition of talc

Formula	Name	Percentage content [%]
SiO_2	Silicon dioxide	64.41
MgO	Magnesium oxide	32.65
CaO	Calcium oxide	2.46
Fe_2O_3	Iron(III) oxide	1.05
Al_2O_3	Aluminium oxide	0.38

The SEM results are presented in Fig. 2. The initial ground talc sample exhibited a heterogeneous morphology consisting of irregular micrometre-sized plate-like fragments accompanied by smaller elongated, needle-like, and lamellar particles (Fig. 2a). After thermal treatment, the general mineral-like morphology was retained, although the particles appeared more fragmented and exhibited a broader range of shapes and sizes (Fig. 2b). The HCl-leached sample still contained relatively large plate-like particles surrounded by smaller lamellar fragments, indicating that acid treatment removed the accompanying mineral components without completely destroying the characteristic morphology of the talc phase (Fig. 2c).

A pronounced morphological transformation occurred after alkaline extraction and subsequent silica precipitation. The original micrometre-sized plate-like structures were no longer observed, and the resulting SiO_2 sample displayed a considerably finer and more homogeneous granular morphology (Fig. 2d). The material consisted of small, approximately globular primary particles that formed larger irregular agglomerates. This agglomeration may be associated with the high surface energy of the fine silica particles and interactions between surface silanol groups during drying. Based on the SEM measurements, the apparent size of the primary silica particles was approximately 100 nm, whereas the agglomerates were considerably larger and reached the micrometre scale. This morphological transformation is consistent with the loss of long-range crystalline order observed by XRD for the final SiO_2 sample.

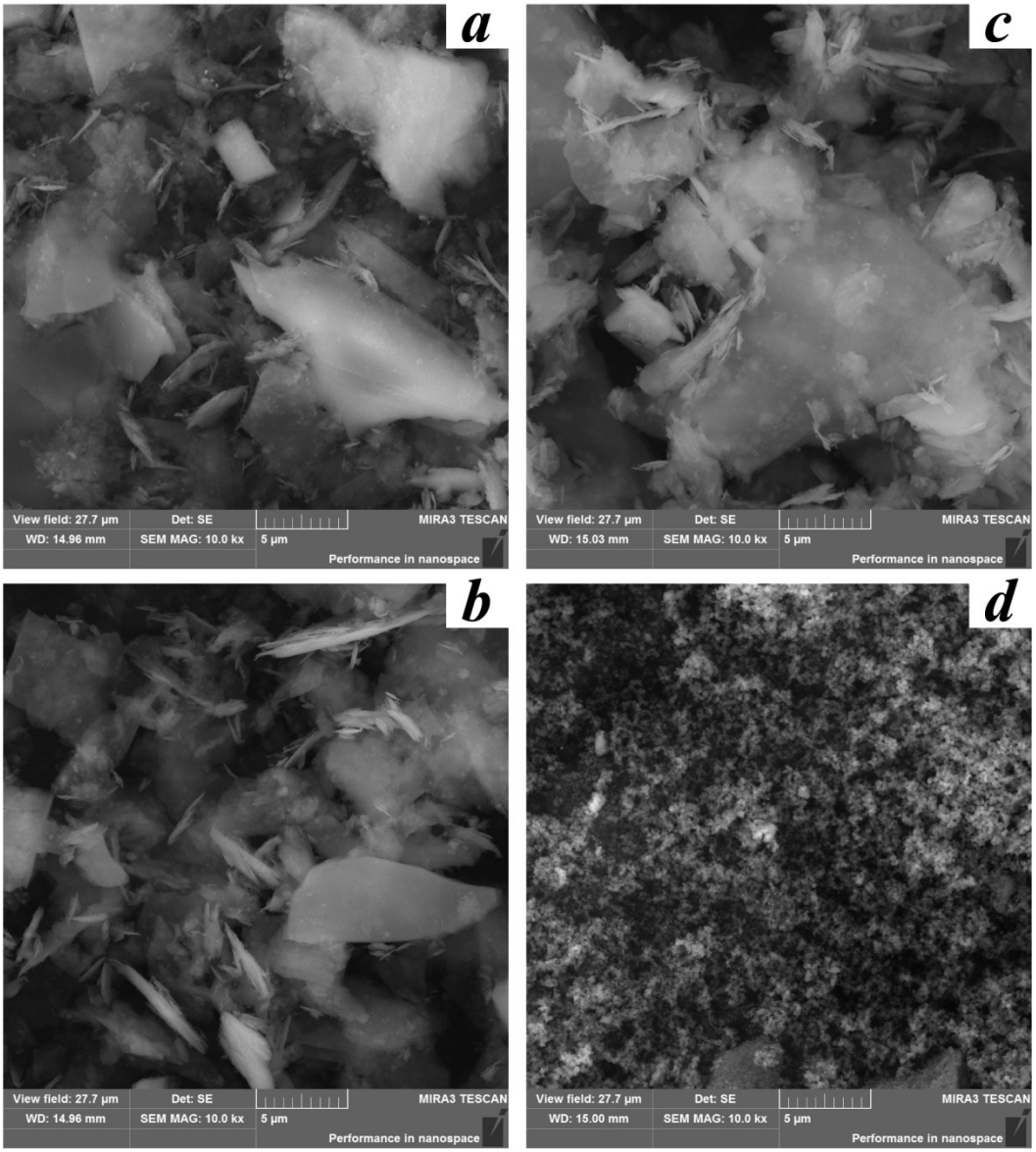

Fig. 2. SEM images of the prepared samples: a – talc after grinding, b – talc after thermal treatment, c – talc after leaching in HCl, d – prepared silica, at 10,000× magnification.

The N_2 adsorption-desorption isotherms and the derived textural parameters are presented in Fig. 3. The initial talc sample had a relatively low specific surface area of 19 $m^2\ g^{-1}$, a total pore volume of 0.066 $cm^3\ g^{-1}$, and a reported pore diameter of 3.4 nm (Fig. 3a). Thermal treatment slightly decreased the specific surface area to 14 $m^2\ g^{-1}$, while the total pore volume increased to 0.080 $cm^3\ g^{-1}$ without a change in the reported pore diameter (Fig. 3b). This suggests that heating did not generate additional accessible surface area but may have caused partial particle rearrangement or densification.

Following HCl leaching, the specific surface area and total pore volume increased moderately to 20 $m^2\ g^{-1}$ and 0.090 $cm^3\ g^{-1}$, respectively, whereas the reported pore diameter increased to 32.4 nm (Fig. 3c). The removal of acid-soluble mineral components therefore appears to have enlarged the voids between the remaining talc particles without producing a highly developed internal surface.

The most pronounced textural changes occurred after alkaline extraction and subsequent precipitation of silica (Fig. 3d). The resulting SiO_2 sample exhibited a specific surface area of 122 $m^2\ g^{-1}$ and a total pore volume of 1.059 $cm^3\ g^{-1}$, corresponding to approximately 6.4- and 16-fold increases, respectively, compared with the initial talc. The reported pore diameter was 32.4 nm. All isotherms displayed a marked increase in N_2 uptake near saturation and an open, H3-like hysteresis loop, indicating that the measured porosity was dominated by large mesopores and interparticle voids associated with aggregates rather than by uniform cylindrical pores. This behaviour was particularly pronounced for the final SiO_2 sample.

The substantial increase in surface area and pore volume can be attributed to the replacement of compact micrometre-sized mineral particles by loosely packed agglomerates of fine silica particles. This interpretation agrees with the SEM observations, which showed the formation of an agglomerated, finely granular morphology after silica precipitation. Thus, the treatment altered not only particle size and morphology but also particle packing and the volume of accessible interparticle voids.

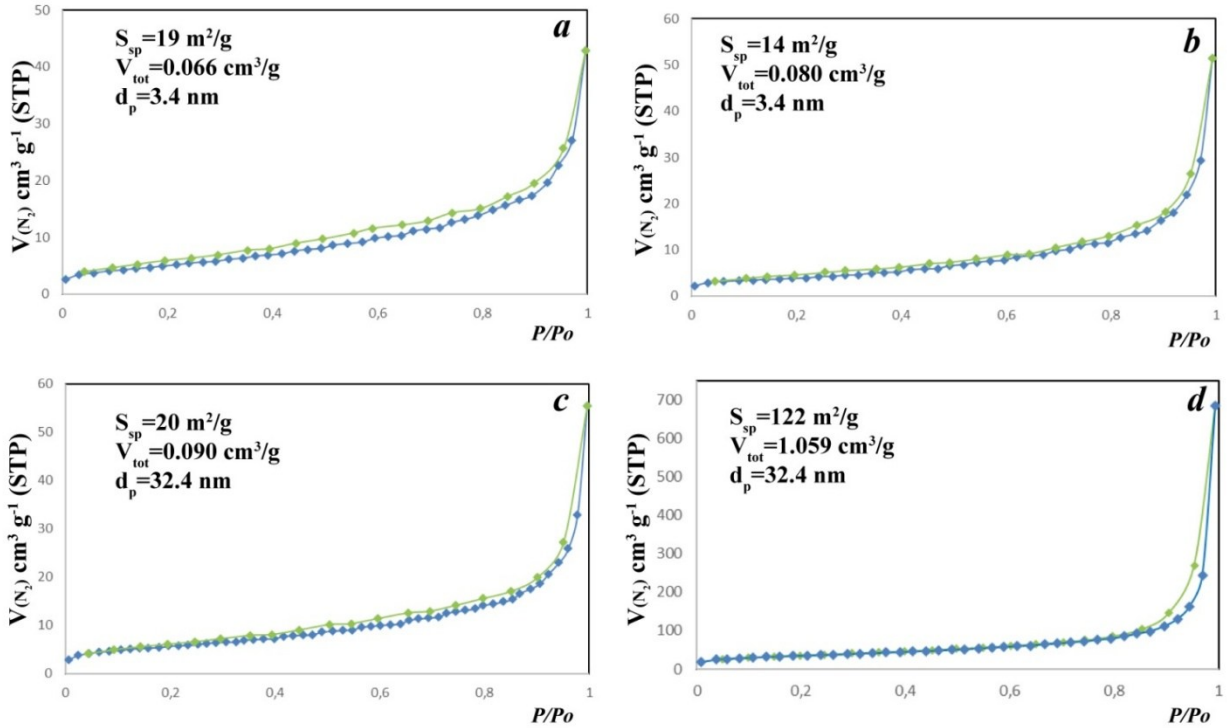

Fig. 2. Nitrogen adsorption–desorption isotherms of the prepared samples: a – talc after grinding, b – talc after thermal treatment, c – talc after leaching in HCl, d – prepared silica (SiO_2).

4. Conclusions

The aim of this work was to prepare silica nanoparticles from talc using a multistep synthesis comprising grinding, thermal treatment, HCl leaching, alkaline extraction, and subsequent silica precipitation. The prepared samples were characterized using several analytical methods to evaluate changes in their structural, morphological, chemical, and textural properties.

XRD analysis showed that talc was the dominant crystalline phase in the initial mineral, accompanied by dolomite, chlorite, and minor graphite. Thermal treatment did not substantially alter the crystalline structure of talc, whereas HCl leaching removed the detectable accompanying crystalline phases. Subsequent alkaline extraction and precipitation produced a material characterized by a broad XRD halo and the absence of sharp Bragg reflections, consistent with the formation of X-ray-amorphous silica without detectable crystalline impurities. The ED-XRF results supported the predominance of talc in the initial material, with SiO_2 and MgO contents of 64.41 and 32.65 wt.%, respectively, and a molar MgO/SiO_2 ratio close to the theoretical value for talc.

A pronounced morphological transformation was also observed. The initial micrometre-sized plate-like and elongated mineral particles were replaced by a finely granular silica structure composed of approximately globular primary particles with an estimated size of about 100 nm. These particles formed larger agglomerates, most likely because of their high surface energy and interactions between surface silanol groups during drying.

The conversion of talc into amorphous silica was accompanied by substantial development of its textural properties. The specific surface area increased from 19 to 122 $m^2\ g^{-1}$, while the total pore volume increased from 0.066 to 1.059 $cm^3\ g^{-1}$. These changes correspond to approximately 6.4- and 16-fold increases, respectively, and indicate the formation of accessible large mesopores and interparticle voids within the silica agglomerates.

Overall, the results demonstrate that the applied treatment sequence effectively transformed the original crystalline talc mineral into finely divided, porous, amorphous silica. The obtained findings confirm that talc can serve as an alternative mineral precursor for the preparation of silica-based materials. The developed silica provides a suitable basis for subsequent surface functionalization and the preparation of adsorbents for inorganic and organic water contaminants. Further studies should focus on optimizing the extraction yield and reagent consumption, evaluating process scalability, and investigating the adsorption performance and regeneration of the resulting functionalized materials.

Acknowledgments

This work was supported by the projects VEGA 2/0138/24 and VAIA 09I03-03-V02-00029, funded by the Recovery and Resilience Plan of the Slovak Republic.

References

1. Ali I. New Generation Adsorbents for Water Treatment. Chemical Reviews, 2012, Vol. 112(10), p. 5073–5091.
2. Burakov A. E. et al. Adsorption of Heavy Metals on Conventional and Nanostructured Materials for Wastewater Treatment Purposes: A Review. Ecotoxicology and Environmental Safety, 2018, Vol. 148, p. 702–712.
3. Diagboya P. N. E., Dikio E. D. Silica-Based Mesoporous Materials: Emerging Designer Adsorbents for Aqueous Pollutants Removal and Water Treatment. Microporous and Mesoporous Materials, 2018, Vol. 266, p. 252–267.
4. Walcarius A., Mercier L. Mesoporous Organosilica Adsorbents: Nanoengineered Materials for Removal of Organic and Inorganic Pollutants. Journal of Materials Chemistry, 2010, Vol. 20, p. 4478–4511.
5. Da'na E. Adsorption of Heavy Metals on Functionalized-Mesoporous Silica: A Review. Microporous and Mesoporous Materials, 2017, Vol. 247, p. 145–157.
6. Marzullo P. et al. Trialkoxysilane Grafting in Alcohols: A Simple Approach towards Modified Silica-Based Materials. Molecules, 2024, Vol. 29(19), 4730.
7. Akhter F. et al. Highly Enhanced Pb(II) Removal by Mercaptopropyl Trimethoxysilane (MPTMS) Surface-Modified Silica Aerogel: Synthesis, Characterization and Isotherm Studies. Physical Chemistry Research, 2024, Vol. 12, p. 219–227.
8. Malafatti J. O. D. et al. Modified Silica Nanoparticles from Rice Husk Supported on Polylactic Acid as Adsorptive Membranes for Dye Removal. Materials, 2023, Vol. 16(6), 2429.
9. Jarvie H. P. et al. Fate of Silica Nanoparticles in Simulated Primary Wastewater Treatment. Environmental Science and Technology, 2009, Vol. 43, p. 8622–8628.
10. Ghani U. et al. Hydrothermal Extraction of Amorphous Silica from Locally Available Slate. ACS Omega, 2022, Vol. 7(7), p. 6113–6120.
11. Petrasová K. et al. Origin and Metamorphic Evolution of Magnesite–Talc and Adjacent Rocks near Gemerská Poloma, Slovak Republic. Journal of Geosciences, 2007, Vol. 52, p. 125–132.
12. Yang H. et al. Preparation of Porous Material from Talc by Mechanochemical Treatment and Subsequent Leaching. Applied Clay Science, 2006, Vol. 31(3–4), p. 290–297.